



The zinc transporter ZIP7 (*Slc39a7*) controls myocardial reperfusion injury by regulating mitophagy

Hualu Zhang¹ · Ningzhi Yang¹ · Haiyan He¹ · Junwu Chai² · Xinxin Cheng¹ · Huanhuan Zhao¹ · Dongming Zhou³ · Tianming Teng⁴ · Xiangrong Kong² · Qing Yang⁴ · Zhelong Xu^{1,3}

Received: 31 May 2021 / Revised: 16 September 2021 / Accepted: 16 September 2021
© Springer-Verlag GmbH Germany, part of Springer Nature 2021

Abstract

Whereas elimination of damaged mitochondria by mitophagy is proposed to be cardioprotective, the regulation of mitophagy at reperfusion and the underlying mechanism remain elusive. Since mitochondrial Zn²⁺ may control mitophagy by regulating mitochondrial membrane potential (MMP), we hypothesized that the zinc transporter ZIP7 that controls Zn²⁺ levels within mitochondria would contribute to reperfusion injury by regulating mitophagy. Mouse hearts were subjected to ischemia/reperfusion *in vivo*. Mitophagy was evaluated by detecting mitoLC3II, mito-Keima, and mitoQC. ROS were measured with DHE and mitoB. Infarct size was measured with TTC staining. The cardiac-specific ZIP7 conditional knockout mice (ZIP7 cKO) were generated by adopting the CRISPR/Cas9 system. Human heart samples were obtained from donors and recipients of heart transplant surgeries. KO or cKO of ZIP7 increased mitophagy under physiological conditions. Mitophagy was not activated at the early stage of reperfusion in mouse hearts. ZIP7 is upregulated at reperfusion and ZIP7 cKO enhanced mitophagy upon reperfusion. cKO of ZIP7 led to mitochondrial depolarization by increasing mitochondrial Zn²⁺ and, accumulation of PINK1 and Parkin in mitochondria, suggesting that the decrease in mitochondrial Zn²⁺ in response to ZIP7 upregulation resulting in mitochondrial hyperpolarization may impede PINK1 and Parkin accumulation in mitochondria. Notably, ZIP7 is markedly upregulated in cardiac mitochondria from patients with heart failure (HF), whereas mitochondrial PINK1 accumulation and mitophagy were suppressed. Furthermore, ZIP7 cKO reduced mitochondrial ROS generation and myocardial infarction via a PINK1-dependent manner, whereas overexpression of ZIP7 exacerbated myocardial infarction. Our findings identify upregulation of ZIP7 leading to suppression of mitophagy as a critical feature of myocardial reperfusion injury. A timely suppression of cardiac ZIP7 upregulation or inactivation of ZIP7 is essential for the treatment of reperfusion injury.

Keywords ZIP7 · Mitophagy · Reperfusion injury · Mitochondrial Zn²⁺ · ROS

Hualu Zhang, Ningzhi Yang, Haiyan He and Junwu Chai contributed equally to this work.

✉ Zhelong Xu
zxu@tmu.edu.cn
Xiangrong Kong
kongxiangrong001@sina.com
Qing Yang
yq1963884@sina.com

- ¹ Department of Physiology and Pathophysiology, Tianjin Medical University, Tianjin 300070, China
- ² Department of Cardiac Surgery, Tianjin First Central Hospital, Tianjin 300192, China
- ³ Department of Pathogenic Biology, Tianjin Medical University, Tianjin 300070, China
- ⁴ Department of Cardiology, General Hospital, Tianjin Medical University, Tianjin 300052, China

Introduction

Although an early restoration of blood flow can improve the survival of ischemic myocardium, it also induces additional injury, a phenomenon termed reperfusion injury [1]. While it is believed that an excessive generation of reactive oxygen species (ROS) from mitochondria are critical for reperfusion injury [2], there is no an efficacious means to prevent mitochondrial ROS generation. Since mitochondria-produced ROS can lead to mitochondrial damage that initiates a feed-forward mechanism of oxidative stress and the cell death pathway, failure to eliminating damaged mitochondria leads to an increased cell death [3, 4]. Therefore, a timely clearance of dysfunctional mitochondria through a specific type of selective autophagy, termed mitophagy [5], is predicted to prevent reperfusion injury [6]. However, the exact status

of mitophagy at reperfusion and the precise mechanism by which mitophagy is controlled at reperfusion remain to be elucidated.

Although exogenous Zn^{2+} has been demonstrated to induce autophagy [7] and mitophagy [8], the roles of zinc transporters that are responsible for the intracellular Zn^{2+} homeostasis in autophagy or mitophagy remain unknown. A recent study showing that the interaction of the zinc transporter ZIP1 with Drp1 promotes mitophagy by reducing mitochondrial membrane potential (MMP) [9] suggest that zinc transporters may play a role in mitophagy. Originally identified through homology to the mouse KE4 gene, the zinc transporter ZIP7 (*Slc39a7*) localizes to the early secretory pathway including Golgi apparatus and ER, and plays a crucial role in intracellular Zn^{2+} homeostasis by tightly controlling movement of the ion into the cytosol from these intracellular vesicles [10]. It has been reported that ZIP7 is involved in tamoxifen-resistant breast cancer progression by activating the growth factor signaling pathways through release of Zn^{2+} from the intracellular stores [11, 12]. ZIP7 also plays a role in B cell development [13], diabetes [10], and ER stress in the heart [14]. Nevertheless, little is known about the role of ZIP7 in the regulation of mitophagy, especially in the setting of cardiac diseases such as myocardial reperfusion injury.

Here, we explored the potential role of ZIP7 in the pathogenesis of myocardial reperfusion injury by determining its regulatory effect on mitophagy as well as mitochondrial ROS generation at reperfusion. We demonstrate that ZIP7 is upregulated at reperfusion and knockout of ZIP7 enhanced mitophagy at reperfusion. Upregulation of ZIP7 reduces mitochondrial Zn^{2+} leading to hyperpolarization, which suppresses mitophagy by preventing PINK1 and Parkin accumulation to mitochondria. Moreover, Cardiac-specific knockout of ZIP7 (ZIP7 cKO) or ZIP7 siRNA reduces ROS generation as well as infarct size in mouse hearts. A timely suppression of ZIP7 upregulation or inactivation of ZIP7 at reperfusion may serve as a cardioprotective strategy not only for the treatment of reperfusion injury but also for the treatment of other cardiac diseases caused by oxidative stress.

Methods

Cell culture and genome editing

Rat heart tissue-derived H9c2 cardiac myoblast cell line was purchased from American Type Culture Collection (ATCC, Manassas, VA, USA). Cells were cultured in culture plates with Dulbecco's modified Eagle's medium (DMEM) (Gibco), supplemented with 10% fetal bovine serum (FBS) (Gibco) and 100 U penicillin/streptomycin at 37 °C in a humidified 5% CO_2 -95% air atmosphere. To generate the

ZIP7 gene knockout (ZIP7 KO) cell line, H9c2 cells were transfected with lentiCRISPRv2 plasmid with a single guide RNA sequence (GCGTGGCTGTGTCCGTGCGCG) using Lipofectamine 3000. This single guide RNA sequence targets exon 4 of *Slc39a7*. After 72 h of transfection, positive cells were sorted by puromycin and seeded at a 96-wells plate to isolate single colonies. Clones were picked when colonies were ~ 100 cells. Colonies were expanded and screened for ZIP7 KO based on disruption of DNA sequence and confirmed by Western blotting.

Hypoxia/reoxygenation (H/R) of H9c2 cells

To induce H/R injury, cells cultured in culture plates filled with DMEM deficient in glucose and FBS were exposed to hypoxia (1% O_2) by placing the plate in a hypoxia chamber (COY Laboratory Products) for 4 h. Then, the hypoxic medium was replaced by the normal DMEM with 10% FBS and cells were cultured in an incubator under normoxic conditions (room air with 5% CO_2) for 2 h.

Animals

Male Wistar rats (250–350 g) and male C57BL/6 mice (8–10 weeks) were purchased from the Institute of Laboratory Animal Science, Chinese Academy of Medical Sciences (Beijing, China). The source of *Slc39a7* (ZIP7) cKO mice is described in this article. All the animal treatments and subsequent analysis were performed in a blind fashion for all groups. All the animal experiment procedures were approved by the Tianjin Medical University Animal Care and Use Committee. All animal experiments described were carried out in accordance with the NIH Guide for the Care and Use of Laboratory Animals (Eighth Edition).

Generation of *Slc39a7* (ZIP7) cKO mice

The cardiac-specific *Slc39a7* conditional knockout mice (ZIP7 cKO) were made in corporation with Nanjing Bio-Medical Research Institute of Nanjing University (NBRI) by adopting the CRISPR/Cas9 system. Transcript *Slc39a7-201* is selected for the presentation of the recommended strategy. *Slc39a7-201* gene has 7 exons, with the ATG start codon in exon1 and TGA stop codon in exon7. Cas9 mRNA, sgRNA and donor were co-injected into zygotes. sgRNA directs Cas9 endonuclease cleavage in intron 2–3 and intron 6–7, and creates a DSB (double-strand break). Such breaks were repaired, and resulted in loxP sites inserted into intron 2–3 and intron 6–7, respectively, by homologous recombination. When mating with cre expression allele, the sequence between two loxP sites can be deleted in specific tissues or cells, disrupting *Slc39a7* gene via frameshift mutation. The correct integration of cre and loxP sites, and the successful

frameshift mutation of *Slc39a7* gene were confirmed by PCR analysis with the primers listed below:

cre-forward: ATACCGGAGATCATGCAAGC.

cre-reverse: AGGTGGACCTGATCATGGAG.

loxP-forward: GTGATGCGTTCCCTCCACCTC.

loxP-reverse: CGTGGTGAGAATGAGGTTCTGC.

Slc39a7-forward: GAAGCTCCATCTTTGCCTTCTG.

Slc39a7-reverse: TTAGGTGGGAGCAGTGTTAAGG.

MHC-MerCreMer induction:

Tamoxifen (Sigma, T5648) was dissolved in corn oil with ethanol (100%) to a concentration of 10 mg/L. Tamoxifen solution was given (75 mg/kg, i.p.) once daily for 3 consecutive days.

Perfusion of isolated rat hearts

Male rats were randomly divided into different groups and anesthetized with sodium pentobarbital (100 mg/kg i.p.). Hearts were removed rapidly and mounted on a Langendorff apparatus and were perfused through a tube connected to a reservoir containing Krebs–Henseleit buffer. A 5–0 silk suture was placed around the left anterior descending coronary artery, and the ends of the suture were passed through a small piece of soft vinyl tubing to form a snare. Hearts were allowed to stabilize for at least 20 min. Hearts were subjected to 30 min regional ischemia followed by 60 min reperfusion.

Isolation of adult mouse cardiomyocytes

Male C57BL/6 mice (8–10 weeks) were given sodium pentobarbital (80 mg/kg, i.p.). Hearts were removed rapidly and mounted on a Langendorff apparatus using a tubing adapter to the aorta. Hearts were perfused in a constant perfusion pressure (90 cm H₂O) with perfusion buffer (120 NaCl, 5.4 KCl, 1.2 NaH₂PO₄, 5.6 Glucose, 20 NaHCO₃, 1.2 MgSO₄, 5 Taurine, 10 2,3-Butanedione Monoxime, in mmol/L) [15] for 4–5 min at a flow rate 2–4 mL/min. When there was ~10 mL of perfusion buffer remaining in reservoir, hearts were perfused with 30 mg collagenase and 0.6 mg protease. After 2 min, remaining buffer in the reservoir was discarded. Hearts were perfused with 6.4 µL 0.25 mmol/L CaCl₂ for 15–20 min. Hearts were cut into two pieces. Then, the hearts were aspirated using a transfer pipet until they fall apart. The supernatants containing dispersed cells were removed into a 50 mL centrifuge tube through a cell strainer, and centrifuge at 500 rpm for 1 min. The supernatants were discarded, and the cell pellets were resuspended with 7 mL of perfusion buffer (containing 5.6 µL 0.25 mol/L CaCl₂ and 0.7 mL bovine calf serum, no more than 10 min). Cells were plated in a dish (pre-coated with L-laminin) with M199 and placed in an incubator.

Mouse heart study

Male mice anesthetized with sodium pentobarbital (80 mg/kg, i.p.) were intubated through a tracheotomy. After opening the chest, the left anterior descending coronary artery (LAD) was surrounded by a 7–0 prolene suture that was then passed through a small plastic tube. Ischemia was induced by tightening the tubing against the heart surface. All hearts underwent 45 min of LAD occlusion followed by reperfusion with different time period, and the sham-operation group was also placed with the suture under the LAD but without occlusion.

Measurement of infarct size

Evans Blue and triphenyltetrazolium chloride (TTC) double staining was used to determine myocardial infarct size at the end of reperfusion. Hearts were excised and sliced. Slices were incubated in 1% TTC at 37 °C for 20 min and fixed with 10% formalin at room temperature. Infarct size was measured with Image J in a single-blind mode and was expressed as a percentage of the risk zone.

siRNA and plasmid transfection in vitro

H9c2 cells with > 80% confluent were transfected with ZIP7 siRNA (Sigma) using Lipofectamine RNAiMAX Reagent (Invitrogen) or plasmid using Lipofectamine 3000 Reagent (Invitrogen) according to the manufacturer's instruction. All experiments were done 48 h after transfection.

siRNA transfection in vivo

Male C57BL/6 mice (8–10 weeks) were injected with 1 OD PINK1 siRNA or ZIP7 siRNA dissolved in 200 µL saline via the tail vein through a 29-gauge needle. Injection was repeated at 8 and 24 h after the first injection. Experiments were conducted 48 h after the first injection. Control mice were injected with saline.

Western blotting analysis

Cardiac cell and tissue homogenates were prepared using RIPA buffer containing 50 mmol/L Tris–HCl, 150 mmol/L NaCl, 0.1% SDS, 1% TritonX-100, and 0.5% Sodium deoxycholate with protease inhibitors (Solarbio, R0010). Equal amounts of protein lysates were loaded and electrophoresed on a SDS–polyacrylamide gel and transferred to a PVDF membrane. Membranes were probed with primary antibodies overnight at 4 °C. Each primary antibody binding was detected with an anti-rabbit (CST, 14,708) or anti-mouse (CST, 14,709) secondary antibody. Proteins were visualized by the enhanced chemiluminescence (ECL) method.

The ECL image was captured with Biospectrum Imaging System (UVP, Upland, CA).

Immunofluorescence staining

After the indicated treatments, live cells or tissue sections were pre-incubated with 200 nmol/L MitoTracker Red CMXRos (Invitrogen M7512) for 30 min at 37 °C. Then, samples were fixed with 4% paraformaldehyde at room temperature, subsequently permeabilized in 0.1% Triton- \times 100/PBS and blocked with normal goat serum (1:10) in PBS for 50 min at 37 °C. The samples were then incubated with primary antibodies against PINK1 (1:100, Novus), ZIP7 (1:100, Invitrogen) and Parkin (1:100, Santa cruz) in PBS overnight at 4 °C. After washing with PBS, the secondary antibodies (anti-Rabbit IgG 488 or anti-Mouse IgG 488, 1:100, Invitrogen) were applied for 1–2 h at room temperature. After washing with PBS, nuclei were stained with DAPI (Beyotime). Samples were imaged with a laser scanning confocal microscope (Olympus FV1200).

Measurement of mitochondrial membrane potential (MMP) in cardiac cells

MMP was detected with JC-1 or TMRE. Cells were loaded with JC-1 (5 mg/ml) or TMRE (0.5 μ mol/L) for 20 min at 37 °C and washed twice with PBS. Fluorescence intensity of cells was detected with confocal microscopy. The green fluorescence of JC-1 monomer was imaged through a 488 nm filter, whereas the red fluorescence of JC-1 aggregation was excited imaged through a 559 nm filter. The ratio between red and green fluorescence was considered a quantitative index of MMP. TMRE fluorescence excited at 550 nm and collected at 574 nm.

Measurement of MMP in isolated mitochondria

Isolated mitochondria loaded with TMRE (0.5 μ mol/L) were treated with 1 μ mol/L TPEN. Changes of fluorescence intensity were detected with a fluorescence plate reader (Molecular Probes) in a time scan mode (TMRE: ex 550 nm, em 574 nm).

Measurement of cardiac ROS

Dihydroethidium (DHE) was used to detect cardiac ROS production in situ [16]. After in vivo experiments, cardiac tissues were embedded in OCT and flash-frozen in liquid nitrogen. Tissues were sectioned at 14 μ m thickness on a cryostat and placed on glass slides. Samples were then incubated with 5 μ mol/L DHE at 37 °C for 15 min and protected from light. After washing with PBS, images were captured using a confocal microscope (Olympus, FV1200). Image J

was used to quantify DHE fluorescence intensity in cardiac sections.

Measurement of mitochondrial hydrogen peroxide (H₂O₂) levels in vivo

Hydrogen peroxide (H₂O₂) levels were measured in living mice using the MitoB probe. MitoB can be targeted at the mitochondrial matrix and oxidized to MitoP by mitochondrial H₂O₂. Both MitoB and MitoP are quantified by high-performance liquid chromatography–tandem mass spectrometer (LC–MS/MS). The ratio of MitoP/MitoB can be used to reflect the level of mitochondrial H₂O₂. Three hours before undergoing ischemia/reperfusion surgery, male C57BL/6 mice (8–10 weeks) were injected with MitoB (0.8 μ mol/kg). After the operation, the heart was flash-frozen in liquid nitrogen and stored at –80 °C for subsequent extraction and quantification of MitoB and MitoP. To extract MitoB and MitoP, the samples were homogenized in a 2.0 mL tube in 500 μ L 60% ACN/0.1% FA. The homogenate was spiked with isotope IS (100 pmol of d₁₅-MitoB and 50 pmol of d₁₅-MitoP), vortexed 30 s, and centrifuged 10 min at 16,000 g. The supernatant was transferred to a fresh tube and the pellet extracted with a further 500 μ L 60% ACN/0.1% FA, which was pooled with the first supernatant. The supernatants were then centrifuged 10 min at 16,000 g, filtered through a 0.22 μ m PVDF filter into a fresh tube. Samples were dried under vacuum using a Savant SpeedVac 2–3 h. The dried samples were resuspended in 150 μ L 20% ACN/0.1% FA by vortexing for 5 min. Finally, the samples were centrifuged 10 min at 16,000 g, and 120 μ L was transferred to an autosampler vial. Samples were then analyzed by LC–MS/MS. For all experiments, a standard curve ($R^2 > 0.99$) was prepared to calculate MitoB and MitoP concentration.

Isolation of mitochondrial fractions

Mitochondrial fractions were isolated by differential centrifugation via a cell mitochondria isolation kit or a tissue mitochondria isolation kit (Beyotime, Shanghai, China) according to the manufacturer's instructions. Cardiac tissues collected from the ischemic zone after the onset of reperfusion in mouse hearts were used for the mitochondrial isolation.

Measurement of intracellular free Zn²⁺

Free Zn²⁺ concentrations in mouse cardiomyocytes were detected with Zinpyr-1 (5 μ mol/L, ChemCruz) according to the manufacturer's instructions. Fluorescence was determined with a confocal microscope.

Measurement of mitochondrial Zn²⁺ concentrations in cardiac tissue

Cardiac mitochondrial fractions were weighed and digested by 1 mL 65% HNO₃ at 120 °C for 30 min. After cooling for 15 min at room temperature, the samples were diluted by mineral-free water. Zn²⁺ was quantified using ICPOES (Perkin Elmer, USA) at a wavelength of 206.200 nm. A multi-element standard solution was used to set up standard curve of Zn²⁺ concentration.

In vivo detection of mitophagy

Mice were injected with 17 µg mito QC plasmid (MRC PPU) via the tail vein 10 h before undergoing LAD occlusion operation. After experiments, mice were perfused with PBS until blood runs clear and switched to 3.7% formaldehyde in 200 mM HEPES, at pH 7.0. Rapidly, excise hearts and postfix at 4 °C overnight. Fixed tissues were washed extensively in PBS at 4 °C, before dehydration with 30% sucrose. The hearts were embedded in OCT and flash-frozen in liquid nitrogen. The tissues were sectioned at 8 µm thickness on a cryostat and placed on glass slides. After washes in PBS, sections were stained with DAPI. Images were captured using a confocal microscope. Image J was used to quantify the mCherry fluorescence.

Mitophagy assay with mKeima

H9c2 cells were transfected with the mKeima-Red-Mito-7 plasmid (Addgene, 56,018) for 48 h. Plasmid transfection was performed as described previously. After treatments, cells were washed twice with PBS and trypsinized. Trypsin was neutralized and cells were pelleted using centrifugation at 1000 rpm for 3 min. Cells were then washed twice in PBS, filtered with a nylon mesh. Fluorescence was determined with the FACSVERGE Flow Cytometer (BD Biosciences, CA, USA). Measurements of lysosomal mKeima were made using dual-excitation ratiometric pH measurements at 488 nm (pH 7) and 561 nm (pH 4) lasers with 527/32 nm and 586/42 nm emission filters, respectively. The FlowJ software was used to assess mitophagy. In the experiments with cardiomyocytes, the mKeima-Red-Mito-7 plasmid was injected into mice and cardiomyocytes were isolated 10 h after the injection. Then, lysosomal mKeima was detected with confocal microscopy.

Human heart samples

Left ventricular and atrial tissue from patients (recipients of heart transplant surgeries) with heart failure (HF) due to ischemic cardiac disease (coronary heart disease) was provided by the Department of Cardiac Surgery, Tianjin First

Central Hospital, Tianjin, China. The study protocol was approved by the Ethics Committee of Tianjin First Central Hospital, Tianjin, China and Tianjin Medical University, Tianjin, China. Atrial myocardium from donor hearts was used as the non-disease control. Informed consents were obtained from all the transplant patients and from the family members of donors before tissue collection.

Statistical analysis

Data are presented as mean ± s.e.m. Number of samples is indicated in figure legends. Statistical analyses were conducted using SPSS17.0. Data were tested for the normality distribution with Shapiro–Wilk test. Statistical significance was determined using the Student's *t* test or one-way ANOVA followed by Tukey's test. *P* values were denoted within each figure panel.

Results

Deficiency or overexpression of ZIP7 induces or inhibits mitophagy under physiological conditions

An excessive generation of ROS especially from mitochondria after the onset of reperfusion is a critical factor for myocardial reperfusion injury. Selective elimination of damaged mitochondria by mitophagy may serve as an effective strategy to prevent excessive generation of ROS from mitochondria [2], since damaged mitochondria enhance production of ROS [17]. ZIP7 can alter MMP, a critical determinant of mitophagy, by moving Zn²⁺ from mitochondria to the cytosol [18]. Therefore we tested the hypothesis that ZIP7 may contribute to the genesis of reperfusion injury by controlling mitophagy. To do this, we first determined the effect of ZIP7 knockout on mitophagy in cardiac H9c2 cells and mouse hearts under normoxic conditions. ZIP7 knockout reduced TOM20, citrate synthase, and P62 expression but increased LC3 II in H9c2 cells, indicating that ZIP7 negatively regulates mitophagy as well as autophagy (Fig. 1a and Fig. S5). Similarly, knockdown of ZIP7 by its siRNA markedly reduced TOM20 expression (Fig. 1b). In support, the cardiac-specific knockout of ZIP7 (ZIP7 cKO) enhanced mitophagy in mouse hearts as indicated by decreases in TOM20, TOM22, and citrate synthase expression but an increase in LC3 II (Fig. 1c and Fig. S5). In contrast, ZIP7 overexpression resulted in an inhibition of mitophagy as indicated by increases in TOM20 and TOM 22 expression but a decrease in LC3 II in mouse hearts (Fig. 1d).

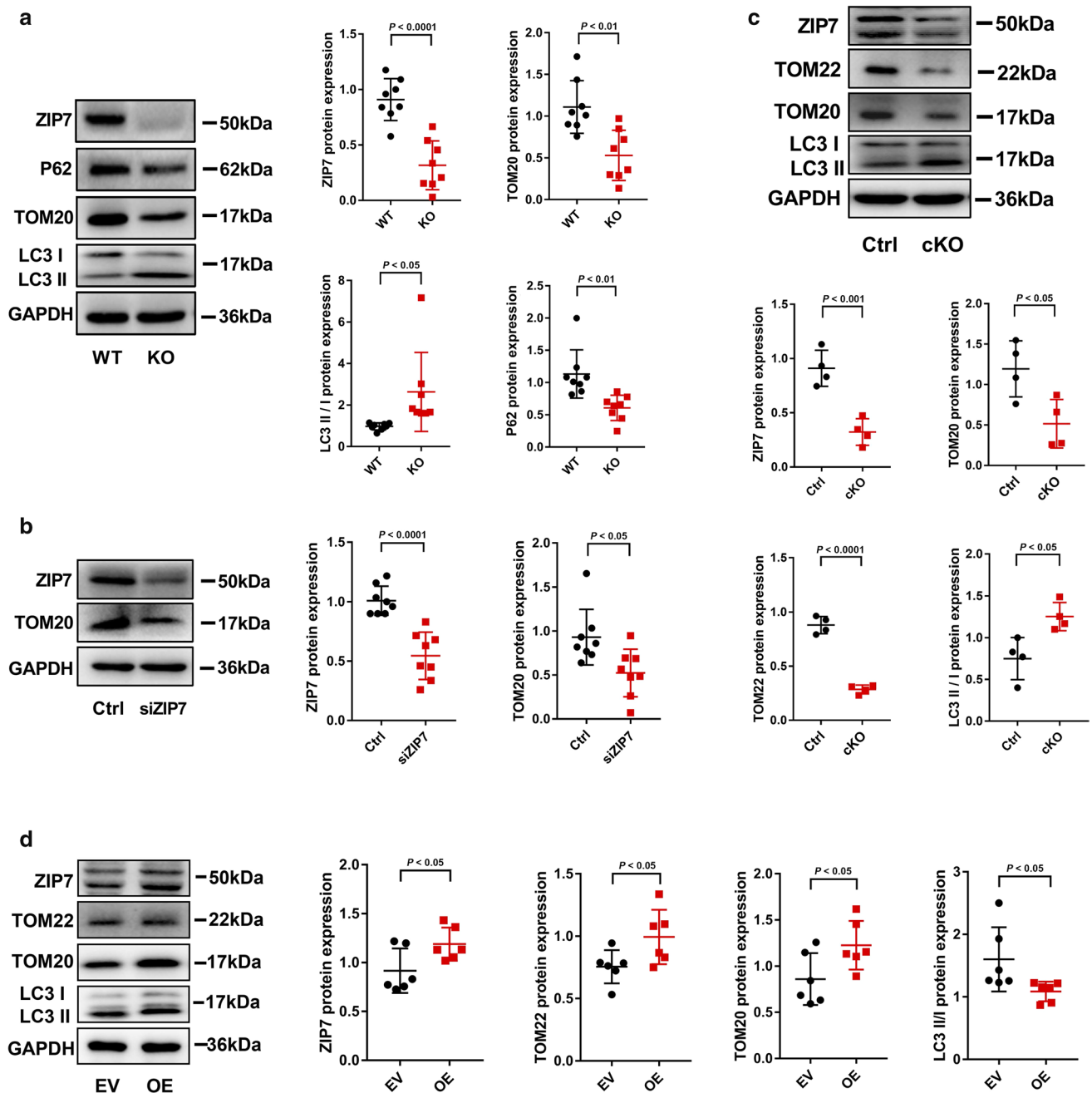


Fig. 1 ZIP7 deficiency induces autophagy as well as mitophagy. **a** Effect of ZIP7 knockout (KO) on P62, TOM20, and LC3II levels in H9c2 cells under normoxic conditions. $n=8$ experiments per group. **b** Effect of ZIP7 siRNA on TOM20 expression in H9c2 cells under normoxic conditions. $n=8$ experiments per group. **c** Effect of ZIP7 cKO on mitophagy assessed by expressions of TOM22, TOM20,

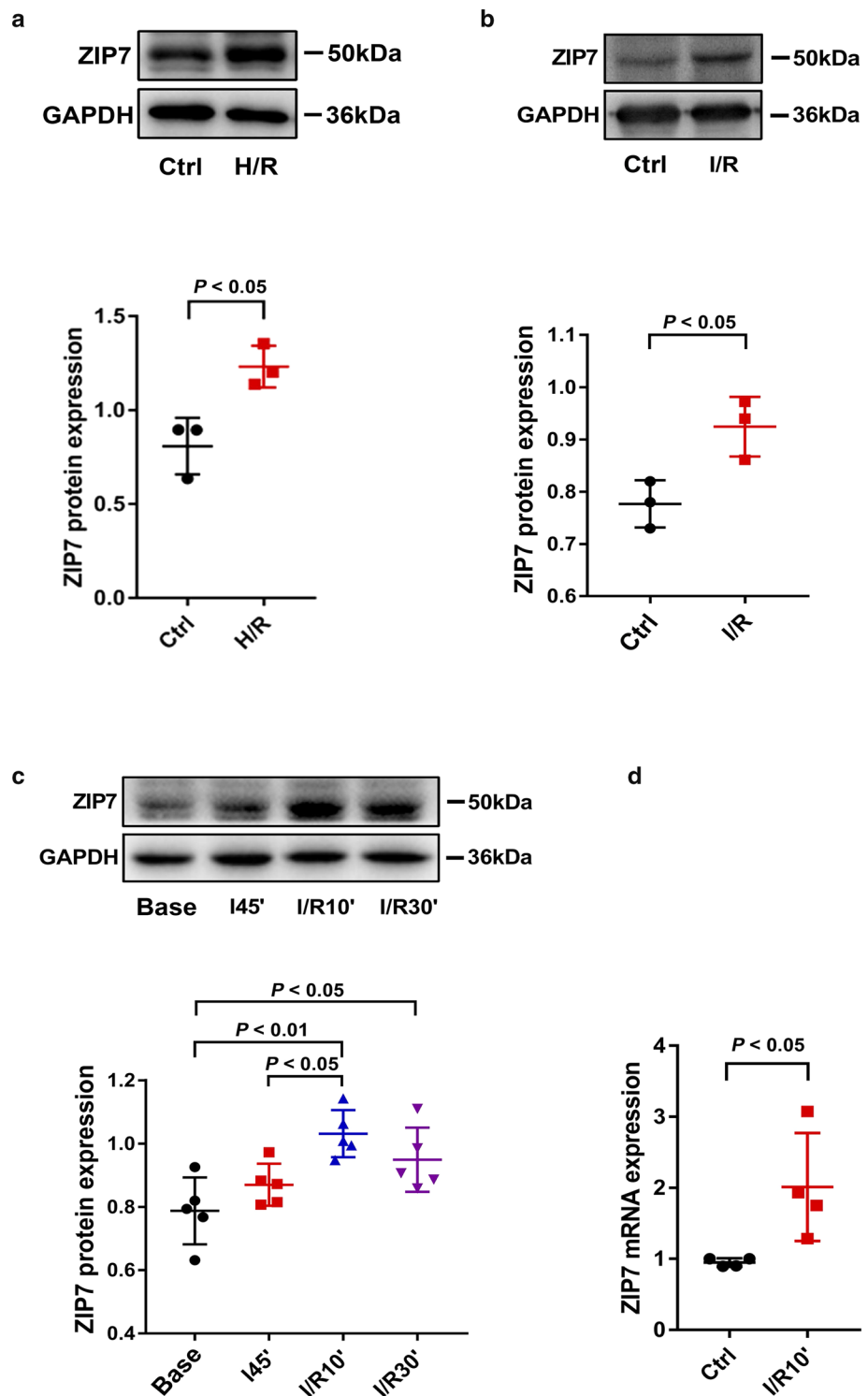
and LC3II in mouse hearts in vivo under normoxic conditions. $n=4$ mice per group. **d** Effect of ZIP7 overexpression (OE) on TOM22, TOM20, and LC3II levels in mouse hearts in vivo under normoxic conditions. *EV* empty vector. $n=6$ mice per group. Data are shown in mean \pm s.e.m. *P* values were determined by Student's *t* test

ZIP7 is upregulated at reoxygenation or reperfusion

Because knockout of ZIP7-induced mitophagy under normoxic conditions, it is possible that changes in ZIP7 expression at reperfusion lead to alteration of mitophagy status. Therefore, we examined if ischemia/reperfusion

(I/R) alters ZIP7 expression. Both hypoxia/reoxygenation (H/R) (isolated mouse cardiomyocytes, Fig. 2a) and I/R (isolated rat hearts, Fig. 2b) significantly increased ZIP7 expression. In particular, ZIP7 was not upregulated at the end of ischemia (45 min) but was markedly increased 10 min after the onset of reperfusion in mouse hearts

Fig. 2 Hypoxia/reoxygenation (H/R) or ischemia/reperfusion (I/R) upregulates ZIP7. **a** ZIP7 expression in isolated mouse cardiomyocytes subjected to 1 h of hypoxia and 30 min of reoxygenation. *n* = 4 mice per group. **b** ZIP7 expression in isolated rat hearts subjected to 30 min of ischemia followed by 60 min of reperfusion. *n* = 3 rats per group. **c** ZIP7 expression in mouse hearts in vivo subjected to 45 min of ischemia (I45') followed by 10 or 30 min of reperfusion (I/R10' or I/R30'). *n* = 5 mice per group. **d** ZIP7 mRNA expression in in vivo mouse hearts subjected to 45 min of ischemia (I45') followed by 10 min of reperfusion (I/R10'). *n* = 4 mice per group. Data are shown in mean ± s.e.m. *P* values were determined by Student's *t* test (**a**, **b**) or one-way ANOVA (**c**)



in vivo (Fig. 2c). Further experiments showed that ZIP7 mRNA expression was also upregulated 10 min after the onset of reperfusion (Fig. 2d). These results prompted us to hypothesize that the upregulation of ZIP7 may play a role during reperfusion by regulating mitophagy.

Deficiency of ZIP7 enhances mitophagy at reperfusion

To demonstrate the above-mentioned hypothesis, we examined the effects of ZIP7 cKO on mitophagy at reperfusion

in mouse hearts *in vivo*. ZIP7, TOM20, and TOM22 expression was increased 10 min after the onset of reperfusion, but this was prevented by ZIP7 cKO (Fig. 3a), indicating that mitophagy is inhibited at the early stage of reperfusion and upregulation of ZIP7 may account for the inhibition of mitophagy. To confirm this observation, we next evaluated mitophagy with mKeima, a sensitive and quantitative fluorophore detecting mitophagy [19, 20], in H9c2 cells or isolated mouse cardiomyocytes. While H/R did not alter mitophagy, ZIP7 KO increased mitophagy either under normoxic conditions or at reoxygenation (left and medium Fig. 3b). Further experiments revealed that ZIP7 cKO led to mitophagy in mouse cardiomyocytes (right, Fig. 3b). To corroborate the effect of ZIP7 on mitophagy *in vivo*, we injected mitoQC plasmid into mice and measured its fluorescence intensity. MitoQC is a pH-sensitive mitochondrial fluorescence probe and displays red and green fluorescence during steady-state conditions, but the mCherry signal becomes stable when mitophagy is induced, because mitochondria are delivered to the lysosome where the GFP signal is quenched [21]. As shown in Fig. 3c, 10 min of reperfusion preceded by 45 min of ischemia did not alter mitophagy. In contrast, ZIP7 cKO markedly enhanced mitophagy 10 min after the onset of reperfusion not only compared to the WT group but also compared to the cKO group at the baseline, implying that ZIP7 is a suppressor of mitophagy at reperfusion. To further confirm that ZIP7 cKO leads to activation of mitophagy, we measured mitochondrial LC3II levels in mouse hearts in the presence or absence of chloroquine. The purity of isolated mitochondrial was identified with tubulin and calnexin antibodies (Fig. 3d). Compared to WT mice, cKO increased mitochondrial LC3II, which was further upregulated by chloroquine, suggesting that ZIP7 cKO activates mitophagy by enhancing the autophagic flow (Fig. 3d). Since ZIP7 is upregulated upon reperfusion (Fig. 2c and Fig. 3b), it is reasonable to propose that mitophagy is supposed to be suppressed by upregulation of ZIP7 at reperfusion. Given that mitophagy inhibition promotes cardiac cell death at reperfusion [6, 20], inhibition of mitophagy by ZIP7 upregulation may contribute to the genesis of reperfusion injury.

Deficiency of ZIP7 leads to Parkin recruitment into mitochondria

Mitophagy is best known to be regulated by the PINK1–Parkin pathway [22]. To test if this pathway is involved in ZIP7 suppression of mitophagy, we measured Parkin and LC3II protein levels in mitochondria isolated from H9c2 cells. ZIP7 KO increased mitochondrial Parkin as well as LC3II, pointing to that ZIP7 KO induces mitophagy by recruiting Parkin into mitochondria (Fig. 4a). Confocal imaging studies also revealed increases in mitochondrial accumulation of Parkin and PINK1 in isolated mouse cardiomyocytes

(Fig. 4b). The specificity of the PINK1 and Parkin antibodies were validated using their siRNAs (Fig. S1). To corroborate these observations, we then conducted experiments with mitochondria isolated from mouse hearts. Similar to the above findings, ZIP7 cKO again increased mitochondrial Parkin, PINK1, and LC3II expression (Fig. 4c). These data together suggest that downregulation of ZIP7 promotes mitophagy through the PINK1–Parkin pathway.

ZIP7 is upregulated but mitophagy is downregulated in patients with heart failure

To confirm the above findings in the clinical situation, we collected heart samples from patients with heart failure (HF) due to ischemic heart disease and measured expression levels of ZIP7, LC3II, and PINK1 in mitochondria. As shown in Fig. 4d, mitochondrial ZIP7 expression was markedly increased in the left ventricle and left atrium of failed hearts compared to the non-disease left atrium. In contrast, mitochondrial LC3II and PINK1 levels were significantly decreased by HF, indicating impaired mitophagy due to the upregulation of ZIP7 in patients with HF. These data are highly consistent with the above findings obtained from mouse hearts.

ZIP7 is localized in mitochondria and deficiency of ZIP7 depolarizes mitochondria by increasing mitochondrial Zn^{2+}

Early studies reported that ZIP7 is predominantly localized to the Golgi apparatus and the ER [23, 24]. However, a recent study demonstrated that ZIP7 is also localized to mitochondria in H9c2 cells and rat cardiomyocytes [25]. This study revealed that ZIP7 is localized to mitochondria in mouse cardiomyocytes and ZIP7 cKO increased mitochondrial Zn^{2+} (Fig. 5a, b). We also found that ZIP7 is localized in mitochondria of mouse hearts (Fig. 5c), which was confirmed by the confocal imaging (Fig. 5c). Furthermore, we demonstrated that mitochondrial ZIP7 was also increased at reperfusion in mouse hearts (Fig. 5d). These data implies that ZIP7 may regulate mitochondrial Zn^{2+} levels at reperfusion. In support, ZIP7 cKO not only increased mitochondrial zinc at baseline but also alleviated I/R-caused zinc loss from mitochondria in mouse hearts (the upper panel, Fig. 5e). ZIP7 cKO also reduced cytosolic zinc loss at reperfusion (the lower panel, Fig. 5e). As ZIP7 increases cytosolic Zn^{2+} by mobilizing Zn^{2+} from intracellular vesicles [18], it is understandable that KO of ZIP7 will lead to an accumulation of Zn^{2+} within mitochondria. Since Zn^{2+} is a cation, its accumulation in mitochondria will lead to mitochondrial depolarization [26], which may induce mitophagy by promoting PINK1 stabilization on the outer membrane of mitochondria. Instead, release of Zn^{2+} from mitochondria

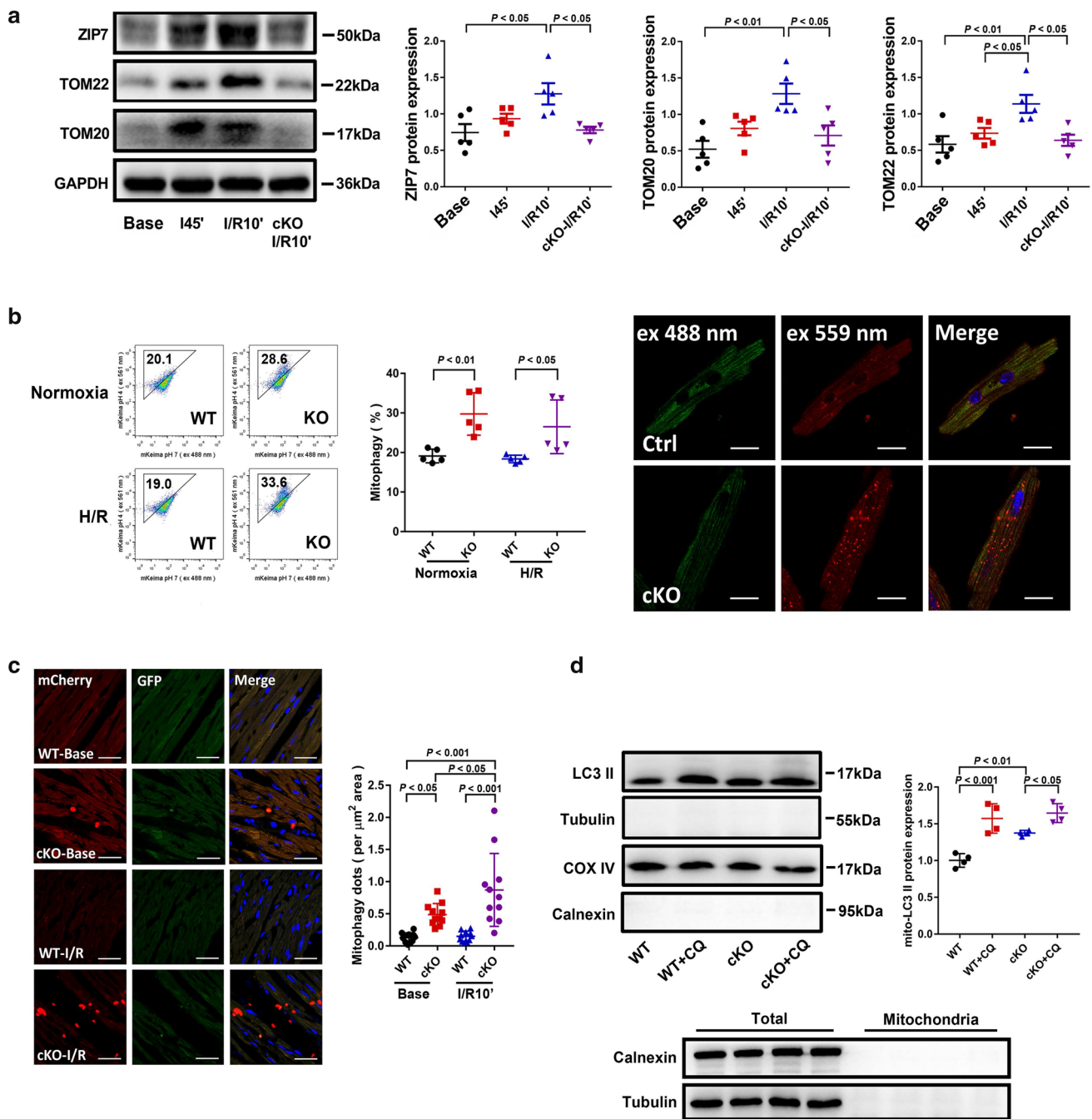


Fig. 3 ZIP7 deficiency promotes mitophagy in the setting of I/R. **a** Effect of ZIP7 cKO on TOM22 and TOM20 expression in mouse hearts in vivo subjected to 45 min of ischemia (I45') and 10 min of reperfusion (I/R10'). $n=5$ mice per group. **b** Effect of ZIP7 KO on mitophagy in H9c2 cells or in mouse cardiomyocytes under normoxic conditions or subjected to 4 h of hypoxia followed by 2 h of reoxygenation (H/R). Mitophagy was analyzed by flow cytometry or confocal microscopy for mKeima. Left, representative flow tracings; middle, quantified data; right, mouse cardiomyocytes. $n=5$ experiments per group in H9c2 cells or $n=3$ mice per group in mouse cardiomyo-

cytes. Scale bar, 20 μm . **c** Effect of ZIP7 cKO on mitophagy in mouse hearts subjected to 45 min of ischemia (I45') and 10 min of reperfusion (I/R10'). Mitophagy was analyzed with confocal microscopy in cardiac sections transfected with mitoQC plasmid. mitoQC plasmid was injected via the tail vein (17 μg). Scale bars, 30 μm . $n=5$ mice per group. Scale bar, 30 μm . **d** Effect of chloroquine on mitochondrial LC3 II levels in mouse hearts. Chloroquine (CQ) was injected intraperitoneally (12 mg/kg). $n=4$ mice per group. Data are shown in mean \pm s.e.m. P values were determined by one-way ANOVA

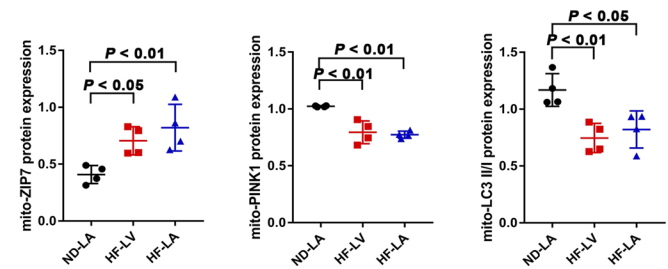
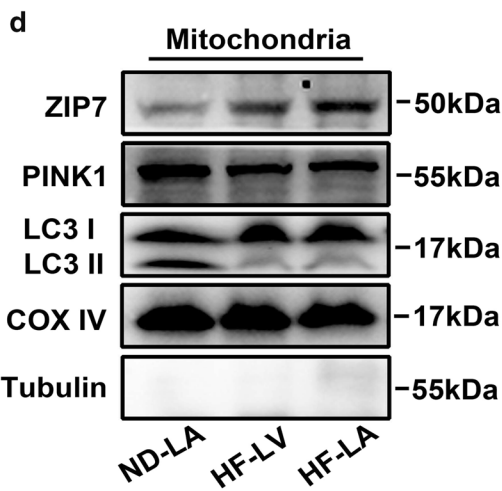
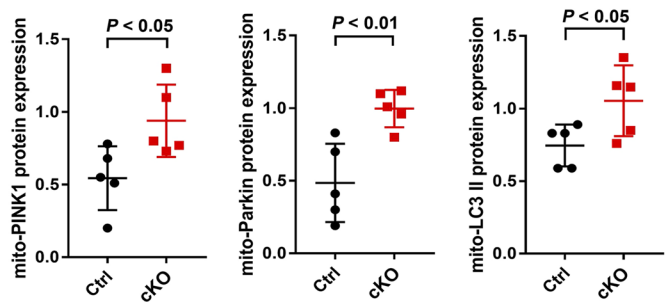
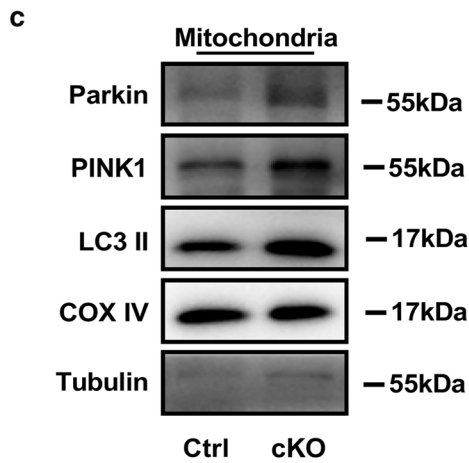
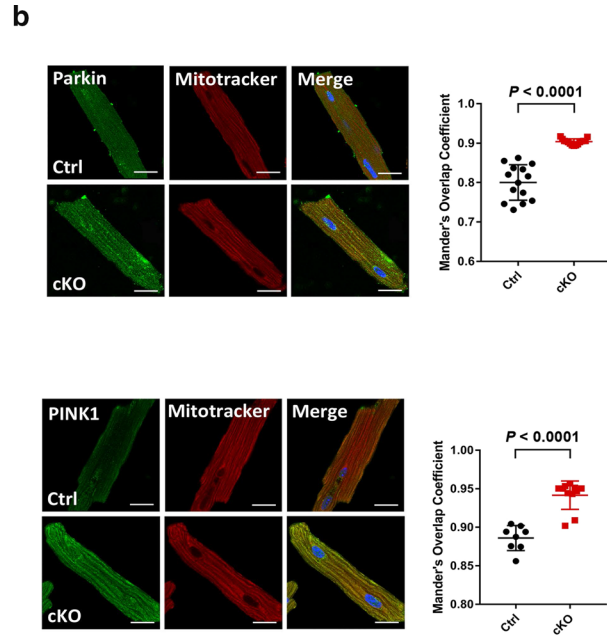
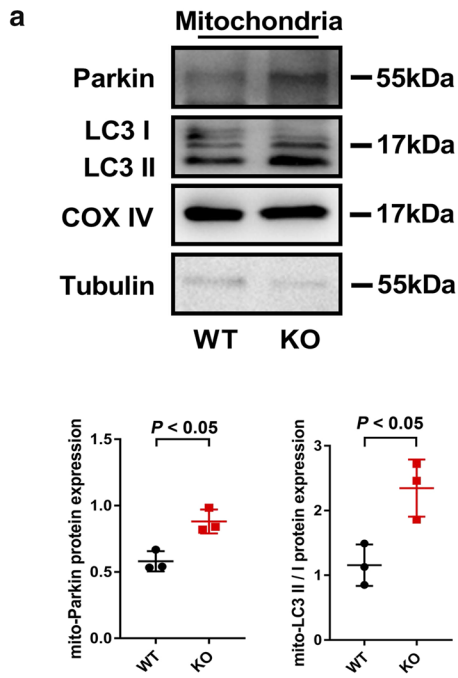


Fig. 4 ZIP7 deficiency increases mitochondrial accumulation of PINK1 and Parkin. **a** Western blotting analysis of Parkin and LC3 expression in mitochondria isolated from H9c2 cells under normoxic conditions. $n=3$ experiments per group. **b** Quantitative colocalization analysis of confocal images of mouse cardiomyocytes. Cardiomyocytes loaded with Mitotracker Red were immunolabeled with Parkin and PINK1. Scale bars, 20 μm . $n=3$ mice per group. **c** Western blotting analysis of Parkin, PINK1 and LC3 expression in mitochondria isolated from mouse hearts under normoxic conditions. $n=5$ mice per group. **d** Western blotting analysis of ZIP7, PINK1 and LC3II expression in mitochondria isolated from human hearts. ND-LA, none-disease left atrium; HF-LV, left ventricle with heart failure; HF-LA, left atrium with heart failure. $n=4$ hearts per group. Data are shown in mean \pm s.e.m. P values were determined by Student's t test (**a–c**) or ANOVA (**d**)

triggered by upregulation of ZIP7 will cause mitochondrial hyperpolarization or diminish the status of depolarization leading to the impediment of PINK1 stabilization. In support, our study revealed that KO of ZIP7 in H9c2 cells resulted in a marked decrease of the aggregation/monomer ratio of JC-1 (left, Fig. 5f), indicating that KO leads to reduction of MMP. Further experiments showed that cKO of ZIP7-induced mitochondrial depolarization as indicated by a decrease in the TMRE fluorescence intensity in mouse cardiomyocytes (right, Fig. 5f). To confirm that the alteration of mitochondrial Zn^{2+} leads to the change of MMP, we measured MMP with TMRE in mitochondria isolated from mouse hearts (Fig. 5g). The Zn^{2+} chelator TPEN was used to downregulate mitochondrial Zn^{2+} . TPEN increased MMP (hyperpolarization) both in WT (left) and in cKO (right) hearts, suggesting that a decrease in mitochondrial Zn^{2+} leads to mitochondrial hyperpolarization. Furthermore, confocal imaging studies showed that the Zn^{2+} level was decreased more sharply than the change of TMRE fluorescence (Fig. S7), indicating that the zinc changes precede the loss of MMP.

Deficiency of ZIP7 reduces ROS production at reperfusion and limits infarct size

One of the most important roles of mitophagy is to prevent oxidative stress by eliminating dysfunctional mitochondria [2]. Accordingly, ZIP7 should regulate ROS generation at reperfusion by controlling mitophagy. In mouse hearts, I/R significantly increased ROS generation, as indicated by an increase in dihydroethidium (DHE) intensity, which was prevented by ZIP7 cKO (Fig. 6a), suggesting that the suppression of mitophagy due to upregulation of ZIP7 is responsible for ROS generation at reperfusion. We next measured mitochondrial H_2O_2 with MitoB in mouse hearts in vivo. MitoB is a mitochondrial targeted spectrometric H_2O_2 probe and has been used to measure mitochondrial H_2O_2 in vivo [27, 28]. Our data showed that I/R increased mitochondrial H_2O_2 , as indicated by an increase in the MitoP/MitoB ratio, and

this was reversed by ZIP7 cKO (Fig. 6b). This result assures us that downregulation of ZIP7 prevents mitochondrial ROS production at reperfusion by enhancing mitophagy.

Because excessive ROS generation from dysfunctional mitochondria is the main determinant of cardiac injury during reperfusion, elimination of dysfunctional mitochondria by mitophagy is supposed to be cardioprotective. Indeed, inhibition of mitophagy promotes cardiac cell death at reperfusion [20], whereas activation of mitophagy is required for simvastatin-induced cardioprotection against I/R [29]. Accordingly, it is reasonable to speculate that alterations of ZIP7 expression may play a role in myocardial I/R injury. In agreement with our assumption, compared to the control, ZIP7 cKO or ZIP7 siRNA significantly reduced infarct size (Fig. 6c). To confirm the role of the PINK–Parkin-mediated mitophagy in the action of ZIP7, we tested if PINK1 siRNA alters the protective effect of ZIP7 cKO. The efficacy of PINK1 siRNA was tested by Western blotting analysis (Fig. S2). As shown in Fig. 6c, the anti-infarct effect of cKO was reversed by PINK1 siRNA. These data suggest that upregulation of ZIP7 contributes to I/R injury through inhibition of mitophagy.

Discussion

We have demonstrated that KO or cKO of ZIP7 enhances mitophagy and reduces mitochondrial ROS generation as well as myocardial infarct size at reperfusion. Since ZIP7 is upregulated upon reperfusion, it is reasonable to propose that ZIP7 plays an essential role in the pathogenesis of myocardial reperfusion injury by suppressing mitophagy resulting in increase of mitochondrial ROS generation and cardiac injury. Our study also identified that downregulation of ZIP7 triggers mitophagy via the PINK1–Parkin pathway. Accumulation of Zn^{2+} within mitochondria caused by downregulation of ZIP7 leads to mitochondrial depolarization, which may account for the activation of the PINK–Parkin pathway. Instead, upregulation of ZIP7 at reperfusion would reduce mitochondrial Zn^{2+} by promoting efflux of the ion, leading to mitochondrial hyperpolarization followed by the inhibition of PINK1 stabilization.

Mitochondria are the primary source of ROS in the heart under pathophysiological conditions [30] and mitochondrial ROS over-generation triggers the mitochondrial permeability transition pore (mPTP) opening followed by mitochondrial depolarization [31]. Subsequently, depolarized mitochondria are removed by mitophagy if the intracellular mitophagic machinery works properly. Instead, failure to remove damaged or depolarized mitochondria due to impaired mitophagy will lead to a vicious cycle of ROS-induced ROS release resulting in cumulative oxidative damage and eventually cardiac cell death [3]. Accordingly, it is

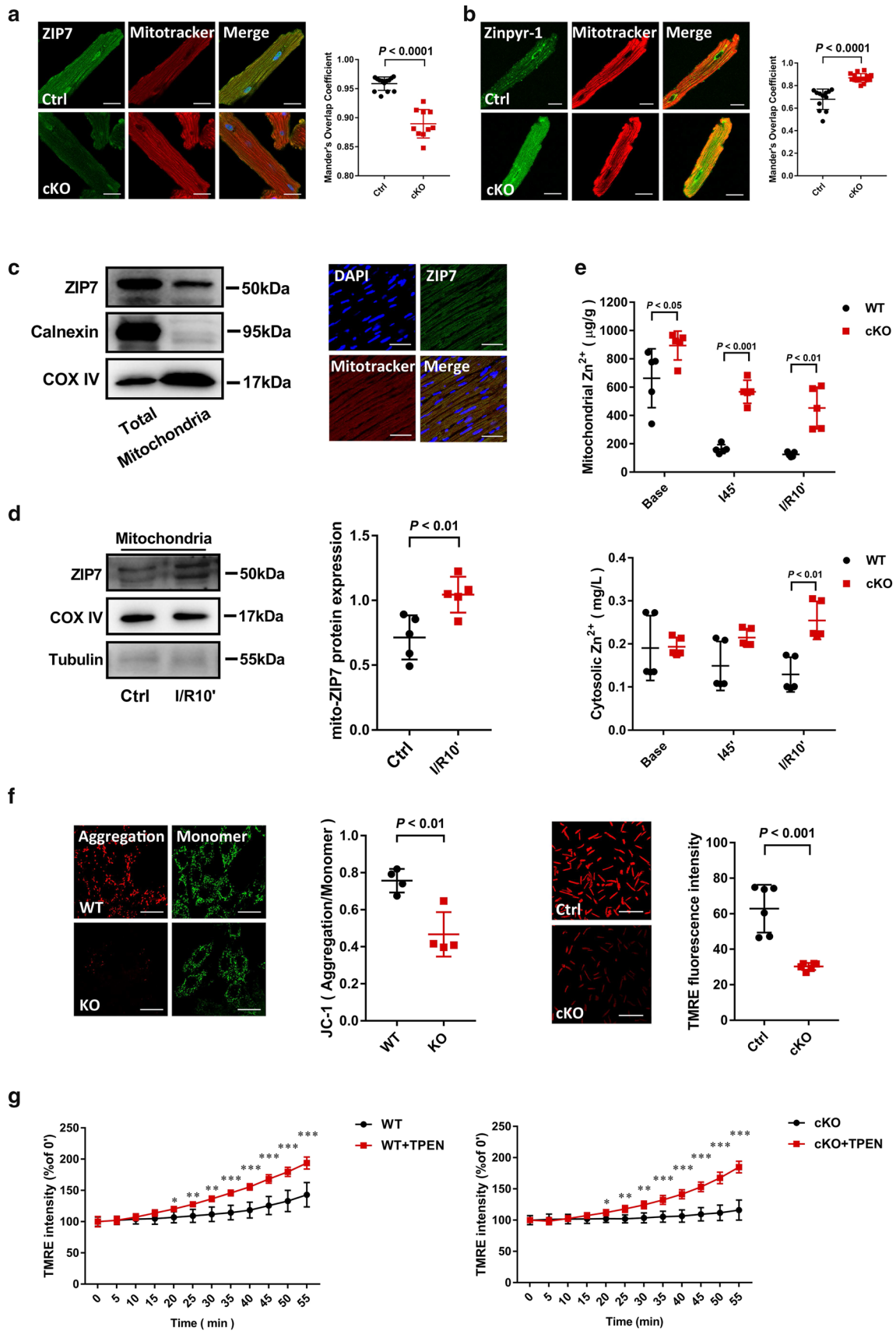


Fig. 5 ZIP7 is localized in mitochondria and deficiency of ZIP7 leads to mitochondrial depolarization by increasing Zn^{2+} accumulation in mitochondria. **a** Detection of ZIP7 in mitochondria in mouse cardiomyocytes by confocal microscopy. Cardiomyocytes loaded with Mitotracker Red were immunolabeled with ZIP7 antibody. $n=3$ mice per group. Scale bars, 20 μm . **b** Confocal images of mouse cardiomyocytes loaded with Zinpyr-1 and Mitotracker Red. $n=3$ mice per group. Scale bars, 20 μm . **c** Detection of ZIP7 in mitochondria by Western blotting (left) and confocal microscopy (right). Mitochondria were isolated from mouse hearts. Heart sections loaded with Mitotracker Red were immunolabeled with ZIP7 antibody. Scale bars, 30 μm . **d** Detection of ZIP7 in mitochondria by Western blotting. Mitochondria were isolated from mouse hearts subjected to 45 min of ischemia and 10 min of reperfusion (I/R10'). $n=5$ mice per group. **e** Mitochondrial (upper) and the cytosolic (bottom) Zn^{2+} levels in mouse hearts measured with ICPOES. Mouse hearts were subjected to 45 min ischemia followed by 10 min of reperfusion (I/R10'). $n=5$ mice per group. **f** Measurements of MMP. H9c2 cells ($n=4$ experiments per group) or mouse cardiomyocytes ($n=3$ mice per group) were loaded with JC-1 or TMRE and analyzed with confocal microscopy. Scale bar, 30 μm . **g** MMP measured with a fluorescence plate reader. Mitochondria isolated from mouse hearts were loaded with TMRE (1 $\mu mol/L$). $n=5$. * $P<0.05$ vs. WT or cKO; ** $P<0.01$ vs. WT or cKO; *** $P<0.001$ vs. WT or cKO. Data are shown in mean \pm s.e.m. P values were determined by one-way ANOVA (**d**), two-way ANOVA (**g**), or Student's t test (**e**)

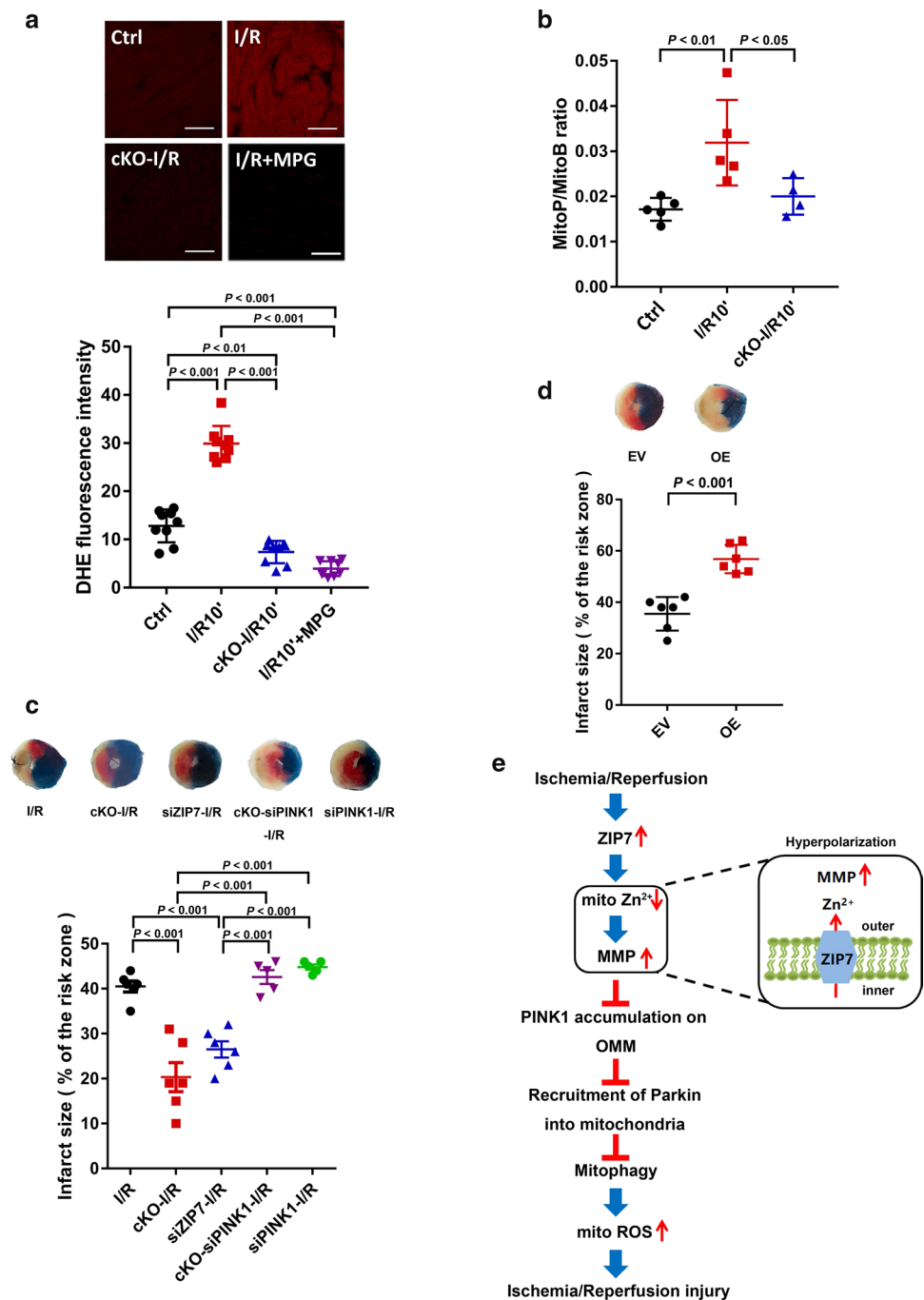
reasonable to speculate that mitophagy is cardioprotective against reperfusion injury. Indeed, inhibition of mitophagy caused by cKO of Drp1 led to accumulation of damaged mitochondria and increased cell death during reperfusion in mouse hearts [20]. In contrast, simvastatin-induced cardioprotection against I/R injury in mouse hearts was mediated by the Parkin-dependent mitophagy [29]. In the present study, we demonstrated that mitophagy is suppressed (Fig. 3a) or at least, is not activated (Fig. 3b, 3c) at early stage of reperfusion in *in vivo* mouse hearts, suggesting that mitophagy is enervated in I/R hearts, which may contribute to myocardial reperfusion injury. Similarly, a recent study demonstrated that mitophagy is inhibited due to decreased LC3 translocation to mitochondria in isolated rat hearts subjected to I/R [32]. It has also been reported that upregulation of MCU contributes to myocardial I/R injury by inhibiting mitophagy [33]. In this study, ZIP7 was upregulated at reperfusion and cKO of ZIP7 enhanced mitophagy. Notably, in human hearts with HF due to ischemic heart disease, mitochondrial ZIP7 expression was increased but mitophagy was suppressed. Moreover, ZIP7 cKO reduced mitochondrial ROS generation as well as infarct size. Likewise, injection of ZIP7 siRNA mimicked the effect of cKO by reducing infarct size. Thus, we propose that upregulation of ZIP7 at reperfusion is the culprit accounting for the inhibition or inactivation of mitophagy at reperfusion and thereby contributing to the genesis of reperfusion injury. Accordingly, a timely and successful heart-specific inhibition of ZIP7 upregulation or inactivation of ZIP7 can protect the heart from reperfusion injury by enhancing mitophagy. However, because knockout

of ZIP7 has also been reported to cause ER stress [34, 35], development of genetic strategies or chemicals that selectively inhibit mitochondrial ZIP7 in the heart is essential for the clinical application. Given that targeting one single mechanism to provide the mitoprotection in the setting of I/R is ineffectual [36] and additive cardioprotective interventions are suggested to produce reliable protection against I/R injury [37], targeting the mitochondrial ZIP7 might be a critical mitoprotective strategy working in concert with the mitoprotective chemicals such as cyclosporine A.

The PINK1/Parkin pathway is one of the best characterized pathway responsible for the induction of mitophagy. The serine/threonine kinase PINK1 is imported into mitochondria, where it is degraded by matrix processing peptidase and presenilin-associated rhomboid-like proteases. However, when mitochondria are depolarized, PINK1 is stabilized and accumulates on the outer mitochondrial membrane. Then, PINK1 induces the mitochondrial recruitment and activation of Parkin [38, 39]. Parkin activation leads to ubiquitination of mitochondrial proteins, promoting the interaction between ubiquitinated proteins and mitophagy receptors/adaptors [40]. In this study, we found that mitochondrial PINK1 and Parkin were increased by either KO or cKO of ZIP7, indicating that upregulation of ZIP7 at reperfusion inhibits mitophagy by preventing PINK1 and Parkin accumulation in mitochondria. Our study with human hearts with HF also confirms these findings. Moreover, the anti-infarct effect of ZIP7 cKO was also reversed by transfection of PINK1 siRNA, confirming the involvement of the PINK1–Parkin pathway in the action of ZIP7.

As described above, PINK1 accumulation on the mitochondrial outer membrane is triggered by mitochondrial depolarization. MMP is regulated by substrate availability, respiratory chain activity, H^+ fluxes, and other ion fluxes than protons [41]. As an important intracellular Zn^{2+} transporter, ZIP7 controls movement of the ion into the cytosol from intracellular vesicles [10, 18]. Our observation that ZIP7 is localized in mitochondria and cKO of ZIP7 leads to increase of Zn^{2+} within mitochondria implies that upregulation of ZIP7 at reperfusion increases Zn^{2+} transport to the cytosol from mitochondria, resulting in a decrease in Zn^{2+} levels within mitochondria. In support, we found that mitochondrial Zn^{2+} was decreased at reperfusion, which was reversed by ZIP7 cKO. Because Zn^{2+} is a cation, the decrease of Zn^{2+} in mitochondria will hyperpolarize mitochondria, resulting in impediment of PINK1 stabilization and accumulation on the mitochondrial outer membrane. In addition, since Zn^{2+} inhibits mitochondrial respiration [42], the decrease of Zn^{2+} in mitochondria will also lead to hyperpolarization by increasing electron transport. Similarly, a recent study demonstrated that the interaction of Drp1 with ZIP1 depolarizes mitochondria by increasing Zn^{2+} entry into mitochondria [9]. Nevertheless, our study revealed no interaction between

Fig. 6 ZIP7 deficiency prevents mitochondrial ROS generation at reperfusion and reduces myocardial infarct size in mouse hearts in vivo. **a** ROS production at reperfusion assessed by DHE staining of mouse heart sections. Mouse hearts were subjected to 45 min ischemia followed by 10 min of reperfusion (I/R10'). Control (Ctrl), no I/R. $n=4$ mice per group. Scale bars, 30 μm . **b** Mitochondrial ROS production at reperfusion in vivo assessed by MitoB oxidation. Mouse hearts were subjected to 45 min ischemia followed by 10 min of reperfusion (I/R10'). Control (Ctrl), no I/R. $n=4-5$ mice per group. **c** Myocardial infarct size assessed by TTC staining. Mouse hearts were subjected to 45 min ischemia followed by 2 h of reperfusion. Top, representative cross-sections of hearts; Bottom, quantification of infarct size. $n=5-6$ mice per group. **d** Myocardial infarct size assessed by TTC staining. Mouse hearts were subjected to 45 min ischemia followed by 2 h of reperfusion. Top, representative cross-sections of hearts; Bottom, quantification of infarct size. $n=6$ mice per group. **e** Proposed model showing how ZIP7 upregulation suppresses mitophagy leading to myocardial I/R injury. Data are shown in mean \pm s.e.m. P values were determined by one-way ANOVA



ZIP7 and Drp1 (Fig. S3). Moreover, other divalent metal ions including Mg²⁺ and Mn²⁺ seem not to be involved in the action of ZIP7 (Fig. S6).

In summary (Fig. 6e), we have demonstrated that upregulation of ZIP7 at reperfusion contributes to the genesis of myocardial reperfusion injury by inhibiting mitophagy at reperfusion. ZIP7 upregulation impedes PINK1 and Parkin accumulation in mitochondria by increasing Zn²⁺ outflow to the cytosol from mitochondria. Our findings obtained both from mouse and human hearts suggest that upregulation of

ZIP7 is an essential signature of myocardial reperfusion injury and that ZIP7 may serve as a novel therapeutic target for myocardial reperfusion injury, and other cardiac diseases caused by oxidative stress or dysfunction of mitochondria. A timely downregulation of the mitochondrial ZIP7 expression or inactivation of the protein may benefit patients with acute myocardial infarction or other cardiac diseases, although its potential for the clinical application needs to be demonstrated by further studies using different animal models (large animals, chronic I/R, etc.) and the validation by

multiple laboratories [43]. Furthermore, because impairment of mitophagy is involved in a number of various diseases such as Parkinson's disease, modulation of ZIP7 expression or activity by pharmacological or genetic approaches may have broad clinical applications. However, it should be mentioned that ZIP7 may also contribute to myocardial I/R injury as a regulator of Zn²⁺ traffic in ER or Golgi apparatus or through its yet unknown effects on mitochondria.

Supplementary Information The online version contains supplementary material available at <https://doi.org/10.1007/s00395-021-00894-4>.

Funding This work was supported by the National Natural Science Foundation of China (NSFC) (grant numbers 81470397, 81970255, and 81802927).

Declarations

Conflict of interest The authors declare no conflict of interest.

References

- Reimer KA, Lowe JE, Rassmussen MM, Jennings RB (1977) The wavefront phenomenon of ischemic cell death. I. Myocardial infarct size vs. duration of coronary occlusion in dogs. *Circulation* 56:786–794
- Kornfeld OS, Hwang S, Disatnik MH, Chen CH, Qvit N, Mochly-Rosen D (2015) Mitochondrial reactive oxygen species at the heart of the matter: new therapeutic approaches for cardiovascular diseases. *Circ Res* 116:1783–1799. <https://doi.org/10.1161/circresaha.116.305432>
- Gottlieb RA, Mentzer RM Jr, Linton PJ (2011) Impaired mitophagy at the heart of injury. *Autophagy* 7:1573–1574. <https://doi.org/10.4161/autof.7.12.18175>
- Saito T, Sadoshima J (2015) Molecular mechanisms of mitochondrial autophagy/mitophagy in the heart. *Circ Res* 116:1477–1490. <https://doi.org/10.1161/circresaha.116.303790>
- Rodríguez-Enriquez S, Kim I, Currin RT, Lemasters JJ (2006) Tracker dyes to probe mitochondrial autophagy (mitophagy) in rat hepatocytes. *Autophagy* 2:39–46. <https://doi.org/10.4161/autof.2229>
- Sciarretta S, Maejima Y, Zablocki D, Sadoshima J (2018) The role of autophagy in the heart. *Annu Rev Physiol* 80:1–26. <https://doi.org/10.1146/annurev-physiol-021317-121427>
- Wei CC, Luo Z, Hogstrand C, Xu YH, Wu LX, Chen GH, Pan YX, Song YF (2018) Zinc reduces hepatic lipid deposition and activates lipophagy via Zn(2+)/MTF-1/PPAR α and Ca(2+)/CaMKK β /AMPK pathways. *FASEB J* 32:6666–6680. <https://doi.org/10.1096/fj.201800463>
- Bian X, Teng T, Zhao H, Qin J, Qiao Z, Sun Y, Liun Z, Xu Z (2018) Zinc prevents mitochondrial superoxide generation by inducing mitophagy in the setting of hypoxia/reoxygenation in cardiac cells. *Free Radic Res* 52:80–91. <https://doi.org/10.1080/10715762.2017.1414949>
- Cho HM, Ryu JR, Jo Y, Seo TW, Choi YN, Kim JH, Chung JM, Cho B, Kang HC, Yu SW, Yoo SJ, Kim H, Sun W (2019) Drp1-Zip1 interaction regulates mitochondrial quality surveillance system. *Mol Cell* 73:364–376.e368. <https://doi.org/10.1016/j.molcel.2018.11.009>
- Adulcikas J, Sonda S, Norouzi S, Sohal SS, Myers S (2019) Targeting the zinc transporter ZIP7 in the treatment of insulin resistance and type 2 diabetes. *Nutrients* 11:408. <https://doi.org/10.3390/nu11020408>
- Taylor KM, Hiscox S, Nicholson RI, Hogstrand C, Kille P (2012) Protein kinase CK2 triggers cytosolic zinc signaling pathways by phosphorylation of zinc channel ZIP7. *Sci Signal* 5:ra11. <https://doi.org/10.1126/scisignal.2002585>
- Taylor KM, Vichova P, Jordan N, Hiscox S, Hendley R, Nicholson RI (2008) ZIP7-mediated intracellular zinc transport contributes to aberrant growth factor signaling in antihormone-resistant breast cancer cells. *Endocrinology* 149:4912–4920. <https://doi.org/10.1210/en.2008-0351>
- Anzilotti C, Swan DJ, Boisson B (2019) An essential role for the Zn(2+) transporter ZIP7 in B cell development. *Nat Immunol* 20:350–361. <https://doi.org/10.1038/s41590-018-0295-8>
- Tuncay E, Bitirim VC, Durak A, Carrat GRJ, Taylor KM, Rutter GA, Turan B (2017) Hyperglycemia-induced changes in ZIP7 and ZnT7 expression cause Zn(2+) release from the sarco(endo)plasmic reticulum and mediate ER stress in the heart. *Diabetes* 66:1346–1358. <https://doi.org/10.2337/db16-1099>
- Baba Y, Higa JK, Shimada BK, Horiuchi KM, Suhara T, Kobayashi M, Woo JD, Aoyagi H, Marh KS, Kitaoka H, Matsui T (2018) Protective effects of the mechanistic target of rapamycin against excess iron and ferroptosis in cardiomyocytes. *Am J Physiol Heart Circ Physiol* 314:H659–h668. <https://doi.org/10.1152/ajpheart.00452.2017>
- Zhang T, Zhang Y, Cui M, Jin L, Wang Y, Lv F, Liu Y, Zheng W, Shang H, Zhang J, Zhang M, Wu H, Guo J, Zhang X, Hu X, Cao CM, Xiao RP (2016) CaMKII is a RIP3 substrate mediating ischemia- and oxidative stress-induced myocardial necroptosis. *Nat Med* 22:175–182. <https://doi.org/10.1038/nm.4017>
- Youle RJ, van der Blik AM (2012) Mitochondrial fission, fusion, and stress. *Science* 337:1062–1065. <https://doi.org/10.1126/science.1219855>
- Lichten LA, Cousins RJ (2009) Mammalian zinc transporters: nutritional and physiologic regulation. *Annu Rev Nutr* 29:153–176
- Hoshino A, Wang WJ, Wada S, McDermott-Roe C, Evans CS, Gosis B, Morley MP, Rathi KS, Li J, Li K, Yang S, McManus MJ, Bowman C, Potluri P, Levin M, Damrauer S, Wallace DC, Holzbaur ELF, Arany Z (2019) The ADP/ATP translocase drives mitophagy independent of nucleotide exchange. *Nature* 575:375–379. <https://doi.org/10.1038/s41586-019-1667-4>
- Ikeda Y, Shirakabe A, Maejima Y, Zhai P, Sciarretta S, Toli J, Nomura M, Mihara K, Egashira K, Ohishi M, Abdellatif M, Sadoshima J (2015) Endogenous Drp1 mediates mitochondrial autophagy and protects the heart against energy stress. *Circ Res* 116:264–278. <https://doi.org/10.1161/circresaha.116.303356>
- Williams JA, Zhao K, Jin S, Ding W-X (2017) New methods for monitoring mitochondrial biogenesis and mitophagy in vitro and in vivo. *Exp Biol Med* (Maywood, NJ) 242:781–787. <https://doi.org/10.1177/1535370216688802>
- Dorn GW 2nd (2016) Jurassic PARK2: you eat your mitochondria, and you are what your mitochondria eat. *Autophagy* 12:610–611. <https://doi.org/10.1080/15548627.2016.1143210>
- Huang L, Kirschke CP, Zhang Y, Yu YY (2005) The ZIP7 gene (*Slc39a7*) encodes a zinc transporter involved in zinc homeostasis of the Golgi apparatus. *J Biol Chem* 280:15456–15463. <https://doi.org/10.1074/jbc.M412188200>
- Taylor KM, Morgan HE, Johnson A, Nicholson RI (2004) Structure-function analysis of HKE4, a member of the new LIV-1 subfamily of zinc transporters. *Biochem J* 377:131–139. <https://doi.org/10.1042/bj20031183>
- Tuncay E, Bitirim CV, Olgar Y, Durak A, Rutter GA, Turan B (2019) Zn(2+)-transporters ZIP7 and ZnT7 play important role in progression of cardiac dysfunction via affecting sarco(endo)plasmic reticulum-mitochondria coupling in hyperglycemic

- cardiomyocytes. *Mitochondrion* 44:41–52. <https://doi.org/10.1016/j.mito.2017.12.011>
26. Devinney MJ, Malaiyandi LM, Vergun O, DeFranco DB, Hastings TG, Dineley KE (2009) A comparison of Zn²⁺- and Ca²⁺-triggered depolarization of liver mitochondria reveals no evidence of Zn²⁺-induced permeability transition. *Cell Calcium* 45:447–455. <https://doi.org/10.1016/j.ceca.2009.03.002>
 27. Chouchani ET, Methner C, Nadochiy SM, Logan A, Pell VR, Ding S, James AM, Cochemé HM, Reinhold J, Lilley KS, Partridge L, Fearnley IM, Robinson AJ, Hartley RC, Smith RA, Krieg T, Brookes PS, Murphy MP (2013) Cardioprotection by S-nitrosation of a cysteine switch on mitochondrial complex I. *Nat Med* 19:753–759. <https://doi.org/10.1038/nm.3212>
 28. Cochemé HM, Quin C, McQuaker SJ, Cabreiro F, Logan A, Prime TA, Abakumova I, Patel JV, Fearnley IM, James AM, Porteous CM, Smith RA, Saeed S, Carré JE, Singer M, Gems D, Hartley RC, Partridge L, Murphy MP (2011) Measurement of H₂O₂ within living *Drosophila* during aging using a ratiometric mass spectrometry probe targeted to the mitochondrial matrix. *Cell Metab* 13:340–350. <https://doi.org/10.1016/j.cmet.2011.02.003>
 29. Andres AM, Hernandez G, Lee P, Huang C, Ratliff EP, Sin J, Thornton CA, Damasco MV, Gottlieb RA (2014) Mitophagy is required for acute cardioprotection by simvastatin. *Antioxid Redox Signal* 21:1960–1973. <https://doi.org/10.1089/ars.2013.5416>
 30. Chen YR, Zweier JL (2014) Cardiac mitochondria and reactive oxygen species generation. *Circ Res* 114:524–537. <https://doi.org/10.1161/circresaha.114.300559>
 31. Crompton M (1999) The mitochondrial permeability transition pore and its role in cell death. *Biochem J* 341:233–249
 32. Chen Q, Thompson J, Hu Y, Dean J, Lesnefsky EJ (2019) Inhibition of the ubiquitous calpains protects complex I activity and enables improved mitophagy in the heart following ischemia-reperfusion. *Am J Physiol Cell Physiol* 317:C910–c921. <https://doi.org/10.1152/ajpcell.00190.2019>
 33. Guan L, Che Z, Meng X, Yu Y, Li M, Yu Z, Shi H, Yang D, Yu M (2019) MCU Up-regulation contributes to myocardial ischemia-reperfusion injury through calpain/OPA-1-mediated mitochondrial fusion/mitophagy inhibition. *J Cell Mol Med* 23:7830–7843. <https://doi.org/10.1111/jcmm.14662>
 34. Bin BH, Bhin J, Seo J, Kim SY, Lee E, Park K, Choi DH, Takagishi T, Hara T, Hwang D, Koseki H, Asada Y, Shimoda S, Mishima K, Fukada T (2017) Requirement of zinc transporter SLC39A7/ZIP7 for dermal development to fine-tune endoplasmic reticulum function by regulating protein disulfide isomerase. *J Invest Dermatol* 137:1682–1691. <https://doi.org/10.1016/j.jid.2017.03.031>
 35. Ohashi W, Kimura S, Iwanaga T, Furusawa Y, Irié T, Izumi H, Watanabe T, Hijikata A (2016) Zinc transporter SLC39A7/ZIP7 promotes intestinal epithelial self-renewal by resolving ER stress. *PLoS Genet* 12:e1006349. <https://doi.org/10.1371/journal.pgen.1006349>
 36. Bøtker HE, Cabrera-Fuentes HA, Ruiz-Meana M, Heusch G, Ovize M (2020) Translational issues for mitoprotective agents as adjunct to reperfusion therapy in patients with ST-segment elevation myocardial infarction. *J Cell Mol Med* 24:2717–2729. <https://doi.org/10.1111/jcmm.14953>
 37. Heusch G (2020) Myocardial ischaemia-reperfusion injury and cardioprotection in perspective. *Nat Rev Cardiol* 17:773–789. <https://doi.org/10.1038/s41569-020-0403-y>
 38. Iguchi M, Kujuro Y, Okatsu K, Koyano F, Kosako H, Kimura M, Suzuki N, Uchiyama S, Tanaka K, Matsuda N (2013) Parkin-catalyzed ubiquitin-ester transfer is triggered by PINK1-dependent phosphorylation. *J Biol Chem* 288:22019–22032. <https://doi.org/10.1074/jbc.M113.467530>
 39. Koyano F, Okatsu K, Kosako H, Tamura Y, Go E, Kimura M, Kimura Y, Tsuchiya H, Yoshihara H, Hirokawa T, Endo T, Fon EA, Trempe JF, Saeki Y, Tanaka K, Matsuda N (2014) Ubiquitin is phosphorylated by PINK1 to activate parkin. *Nature* 510:162–166. <https://doi.org/10.1038/nature13392>
 40. Lazarou M, Sliter DA, Kane LA, Sarraf SA, Wang C, Burman JL, Sideris DP, Fogel AI, Youle RJ (2015) The ubiquitin kinase PINK1 recruits autophagy receptors to induce mitophagy. *Nature* 524:309–314. <https://doi.org/10.1038/nature14893>
 41. Wikstrom JD, Twig G, Shirihai OS (2009) What can mitochondrial heterogeneity tell us about mitochondrial dynamics and autophagy? *Int J Biochem Cell Biol* 41:1914–1927. <https://doi.org/10.1016/j.biocel.2009.06.006>
 42. Brown AM, Kristal BS, Efron MS, Shestopalov AI, Ulluca PA, Sheu KFR, Blass JP, Cooper AJL (2000) Zn²⁺ inhibits alpha-ketoglutarate-stimulated mitochondrial respiration and the isolated alpha-ketoglutarate dehydrogenase complex. *J Biol Chem* 275:13441–13447. <https://doi.org/10.1074/jbc.275.18.13441>
 43. Lecour S, Andreadou I, Bøtker HE, Davidson SM, Heusch G, Ruiz-Meana M, Schulz R, Zuurbier CJ, Ferdinandy P, Hausenloy DJ, Adamovski P, Andreadou I, Batirel S, Barteková M, Bertrand L, Beauloye C, Biedermann D, Borutaite V, Bøtker HE, Chlopicki S, Dambrova M, Davidson S, Devaux Y, Di Lisa F, Djuric D, Erlinge D, Falcao-Pires I, Ferdinandy P, Galatou E, Garcia-Sosa A, Girao H, Giricz Z, Gyongyosi M, Hausenloy DJ, Healy D, Heusch G, Jakovljevic V, Jovanic J, Kararigas G, Kerkal R, Kolar F, Kwak B, Leszek P, Liepinsh E, Lonborg J, Longnus S, Marinovic J, Muntean DM, Nezcic L, Ovize M, Pagliaro P, Da Costa Gomes CP, Pernow J, Persidis A, Pischke SE, Podesser B, Potočnjak I, Prunier F, Ravingerova T, Ruiz-Meana M, Serban A, Slagsvold K, Schulz R, van Royen N, Turan B, Vendelin M, Walsh S, Zidar N, Zuurbier C, Yellon D, on behalf of the European Union CCAC (2021) Improving preclinical assessment of cardioprotective therapies (IMPACT) criteria: guidelines of the EU-CARDIOPROTECTION COST action. *Basic Res Cardiol* 116:52. <https://doi.org/10.1007/s00395-021-00893-5>